Azimuth Resolution Improvement for Squinted Synthetic Aperture Radar Imaging Based on Matched Slope Filter

Farhad Sadeghi Almaloo[1], Majid Zarie[1], Khodadad Halili[2], and Jafar Khalilpour[1]
[1] Electrical Engineering Department, Khatam al-anbia (pbuh) University, Tehran, Iran
[2] Shahid Sattari Aeronautical University of Science and Technology, Tehran, Iran
Email: farhad.sadeghi@srbiau.ac.ir; majidzarie@yahoo.com; {kh.halili; j-khaliepour}@ssau.ac.ir

***Abstract*—Improving the resolution of Synthetic Aperture Radar (SAR) is a major issue that has gained significant attention recently, especially in the squint mode where obtaining high resolution is challenging. Generally speaking, the azimuth and range resolutions can be improvement by applying matched filtering for compressing the signal. Signal compression is a major part of the well-known algorithms such as the Range Doppler algorithm (RDA) and the Chirp Scaling Algorithm (CSA) by which high positioning accuracy and high resolution are obtained. The transmitted signal by SAR is most often in the form of linear frequency modulation (LFM). However, the chirp signal is always generated in the SAR azimuth direction at the receiver. The squint of observation angle of the radar makes the chirp signal non-linear and non-stationary. Consequently, this study particularly focuses on the azimuth signal compression and instead of the Matched Filter (MF) based on Fourier Transform (FT), an alternative Matched Filter is used for signal compression on time-frequency domain that is known as Matched on Slope Filter (MSF). The Matched on Slope Filter improves the effectiveness of the compression in both squint and non-squint modes. The simulation results indicate that the proposed method improves the resolution and decreases the Peak to Side Lobe Ratio (PSLR) in the target detection.**

***Index Terms*—Squinted SAR, matched on slope filter, azimuth resolution, signal compression, fractional Fourier transform**

I. Introduction

Recently, Synthetic Aperture Radar (SAR) has been extensively used in various military and non-military applications for providing high-resolution images from the earth's surface using electromagnetic waves during day and night and under different weather circumstances. Examples include remote sensing, mine and oil exploration, jungle and climate changes observation, and surface object detection. To obtain high-resolution images in SAR, the resolution is defined in two dimensions, including "range" and "azimuth", where the azimuth direction is orthogonal to the range direction. The methods to achieve range resolution are the same on all radars, but the improvement of azimuth resolution by processing algorithms is only discussed in SAR. In this paper, it is assumed that range resolution has been achieved by conventional methods and only azimuth resolution improvement has been considered. Most of the SARs, especially those used in airborne, use squint imaging since it delivers higher flexibility in their applications. For instance, spotlight SAR should capture images in the squinted mode. In fact, processing signals along the azimuth direction is the most important difference between SAR and other kinds of radars. Specifically, when squinted imaging is adopted, increasing the resolution in the azimuth direction becomes a challenging issue. Here, phase changes are increased hence higher phase compensation should be applied in the RCMC algorithm [1], [2]. The main part of the SAR signal processing algorithms, such as the Range Doppler Algorithm (RDA) and the Chirp Scaling Algorithm (CSA), is the signal compression, especially the azimuth signal compression. Signal compression in SAR is conducted using matched filtering. A matched filter used in the processing algorithms should be applied to the received echo signals in the range direction and to the signal in the azimuth direction; hence, in addition to more accurate positioning of the targets, it enhances the resolution of detecting multiple close targets [3]–[5].

Resolution quality is shown to be directly related to the bandwidth of the transmitted signal by the radar [4]. A high bandwidth in the range direction can be supplied by the emitted signal by the radar to improve the range resolution. In the azimuth direction, increasing target's Doppler bandwidth or increasing target's Doppler history increases the azimuth resolution. It has been shown that increasing the Doppler bandwidth in SAR is not related to the transmitted waveform by the radar [3], [5]. Instead, a higher Doppler bandwidth can only be achieved by increasing the length of the synthetic aperture. Further, a large synthetic aperture is achieved by moving the radar along a trajectory, which can be done by placing the radar on an airplane or a satellite. As discussed in these sections, after receiving the reflected echo from a target in a SAR receiver, regardless of the transmitted

Manuscript received January 2, 2020; revised April 1, 2020; accepted April 15, 2020.

Corresponding author: Farhad Sadeghi Almaloo (email: farhad.sadeghi@srbiau.ac.ir).

doi: 10.18178/ijeetc.9.6.390-398

waveform, the detected azimuth component in the signal is nearly a Linear Frequency Modulation (LFM) signal. Therefore, LFM signal is among the signals transmitted by SAR that has a diagonal characteristic in the time-frequency plane and it is employed in SAR because of its wide bandwidth that can be exploited to improve the range resolution. In addition, the azimuth signal is inherently a pseudo-LFM signal. Thus, implementing a matched filter in SAR for an LFM signal is crucial. Although the resolution quality in this kind of radar is a function of bandwidth of the transmitted signal and target exposure time or target's Doppler history, higher resolutions can be achieved by employing processing methods and effective LFM signal compression algorithms in both range and azimuth directions. Given the above discussion, the present paper studies the azimuth pseudo-LFM signal compression in squint SAR imaging by using matched filters, aiming at improving the azimuth resolution. Moreover, the achieved results of the proposed method in this study can simply be applied in SAR signal processing algorithms such as the RDA and CSA to simultaneously improve the range resolution.

Implementing matched filtering using the Fourier Transform (FT) is considered as a traditional compression method in the frequency domain [6]. In the present paper, an alternative method is proposed, which is based on the fractional Fourier transform (FrFT). Both the traditional method and the proposed method were simulated and compared to show the benefits of the proposed method. The FrFT method has gained attention during the last decade; it has been successfully deployed in various areas such as optics, nuclear physics and signal processing. The FrFT appeared within mathematical literature long time ago; its introduction goes decades back when Namias introduced it in the 1980s and later employed in optics applications. Further, recently, the FrFT has been considered as a powerful signal processing tool, especially in radar signal processing and compression [7]–[9]. Elgamel *et al*. employed matched filters based on the FrFT for the chirp signal compression [10]. The authors applied the Principle of Stationary Phase (POSP) of a chirp signal and showed that the compression rate of a chirp signal depends on factors such as the duration of the pulse containing the chirp and bandwidth of the chirp signal. They also showed that employing the FrFT can yield better compression than that of the FT, provided that the chirp parameters are correctly predicted. Further, Amein *et al*. developed the CSA based on the FrFT [11]. In their proposed method, Range Cell Migration Correction (RCMC) is used for phase compensation of the signal and position correction of the target in range cells. They applied RCMC in the FrFT domain by applying a proper phase within each range cell. In addition, Xiao *et al*. enhanced the RDA algorithm for high squinted SAR [12]. The authors applied the RCMC for phase compensation in the FT domain within two steps. In the first step, compensation with linear steps is conducted, and in the second step, the compensation of non-linear parts of the RCMC is dealt with. The simulation results indicated that only Peak to Side Lobe Ratio (PSLR) was reduced in their method. Clemente *et al*. and Mashed *et al*. adopted the same methods in the RDA algorithm with the FrFT in the presence of Gaussian white noise [13], [14]. Their simulation results revealed that the proposed method has an insignificant impact on the resolution and only reduces PSLR. Similarly, the simulation results presented in indicated resolution degradation and false target detection along with the actual target [14]. Chen *et al*. extended the CSA algorithm in the squinted mode using the FrFT [15]. The authors applied a preprocessing step, called Linear Range Walk Correction (LRWC), as a primary compensation step with linear steps. LRCW is applied before applying the main phase compensation and the FrFT-based CSA algorithm. The preprocessing step is performed by applying the FrFT under 90 ° angle. The FrFT under 90 ° angle equals the FT. Thus, their method is basically similar to the method presented by Amein & Soraghan, 2006, in which a primary phase compensation step is added. Fan *et al*. simulated the same method but by using the FFT [6]. The results of both methods demonstrated that the resolution was unchanged and only PSLR was reduced.

In the proposed method, a Matched on Slope Filter (MSF) and location scaling along the azimuth direction is exploited to improve the resolution and PSLR through maximal compression of the azimuth SAR signal at the Doppler centroid. What differentiates the azimuth SAR signal from the LFM signal along the range direction in radars is the properly pseudo-linear of the azimuth signal since the time-frequency characteristic of the signal along the synthetic aperture is not completely linear, and the frequency variation at different points of the characteristic is not constant. What is more, in the case of squinted imaging, the range direction also exhibits phase changes and the RCM becomes non-linear and a function of the azimuth phase [2], [12]. Here, it is impossible to compress the range signal under a constant chirp rate. The FrFT allows the matched filter (MF) to be applied according to the Slope changing of the time-frequency characteristic when the chirp rate in the pseudo-LFM signal is variable. Thus, the FrFT is tailored for processing signals with a non-linear frequency characteristic as well as LFM signals.

The main contributions of this work can be summarized as follows:

- We have proposed a new type of two-dimensional MF as called Matched on Slope Filter (SMF) to find the target location. In the other works, MF is implemented only in the frequency (or time) domain, by which the correlation between the received signal and the reference signal is measured. In our proposed method using FrFT, the correlation between these is measured by their time-frequency Slope characteristic. In other words, the highest correlation occurs when the Slopes of their characteristic are equal. Applying FrFT in the other works is different from ours. They used FrFT to compensate for the phase of the received signal and implemented MF using FT [3], [5], [8], [10], [11], [13], [16].

- In our proposed method it is possible to calculate the Slope of the time – frequency characteristic locally. Consequently, if the Slope is changed nonlinearly, the Slope of the time- frequency characteristic can be calculated at any time. This enables non-stationary processing.
- In our work, (slow) time-frequency coordinates converts to a new (slow) time- frequency coordinates and after locating targets on the (slow) time axis, the position of the targets is transferred to their actual location with a linear transformation, which is only a function of FrFT parameter (angle of transform). As a result, the implementation of the MSF is simple and similar to MF.
- The proposed method is robust to squint signal variations while in the target detection based on the usual Matched Filter the resolution decreases by increasing the squint angle.

The content of the paper is presented as follows. FrFT is briefly introduced and some of its important properties in signal processing are reviewed. Next, the model of the azimuth imaging system and the theory of signal reconstruction is discussed succinctly. Then, the traditional signal compression method based on the FFT and our novel method for signal compression based on the FrFT is introduced; the simulation results are presented.

II. FRFT AND ITS APPLICATION IN SIGNAL PROCESSING

The Fourier Transform (FT) is a mapping operation from a one-dimensional signal in the time domain $x(t)$ to a one-dimensional frequency spectrum $X(f)$. If the FT is expressible in a two-dimensional with perpendicular time-frequency axes, after applying the FT, the signal in the time domain is mapped onto the frequency spectrum by $\pi/2$ clockwise rotation. Therefore, after applying the FT, the time information about the frequency spectrum components of the signal is eliminated, thereby reducing time analysis capability of the signal, especially in the case of non-linear signals.

The FrFT transform, as a linear Time-Frequency Representation (TFR), is a more general form of the FT, in which the rotation angle of the time-frequency characteristic of a signal can be an arbitrary value denoted by α, instead of a fixed value of 90°. In other words, in this kind of transformation, the characteristic of a time signal in the time-frequency plane can be mapped onto the frequency axis under any arbitrary angle. In this way, both time and frequency information of the signal are available at the same time. The FrFT of a signal denoted by $x(t)$ under the rotation angle of α degrees is defined as follows:

$$X_a(u) = \int_{-\infty}^{\infty} x(t) K_a(t,u)\, dt \tag{1}$$

where $\alpha = a/2$. a is the order of transformation and $K_a(t,u)$ is called the main transformation kernel; it is defined as:

$$K_a(t,u) = \begin{cases} \sqrt{\dfrac{1-j\mathrm{cotg}\alpha}{2\pi}} \exp\left(j\dfrac{t^2+u^2}{2}\mathrm{cotg}\alpha - jtu\cdot\csc\alpha \right), & \alpha \neq n\pi \\ \delta(t-u), & \alpha = 2n\pi \\ \delta(t+u), & \alpha = (2n+1)\pi \end{cases} \tag{2}$$

Considering the above equations, the following can be inferred:

$$a = 1 \Rightarrow X_a(u) = X(+f)$$
$$a = 2 \Rightarrow X_a(u) = X(-t)$$
$$a = 3 \Rightarrow X_a(u) = X(-f)$$
$$a = 4 \Rightarrow X_a(u) = X(+t)$$

The range of FrFT in the time-frequency (*t-f*) plane is shown in Fig. 1. In fact, the transforming order *a* as a degree of freedom, creates a new intermediate domain between time and frequency domains, called the FrFT domain, as illustrated in Fig. 2.

As it can be observed from the figure, the new time and frequency axes, i.e. *u* and *v*, maintained their orthogonality after the transformation. The inverse FrFT transformation can be obtained by taking the FT under the rotation angle of $-\alpha$:

$$x(t) = \int_{-\infty}^{\infty} x_a(u) K_{-a}(t,u)\, dt \tag{3}$$

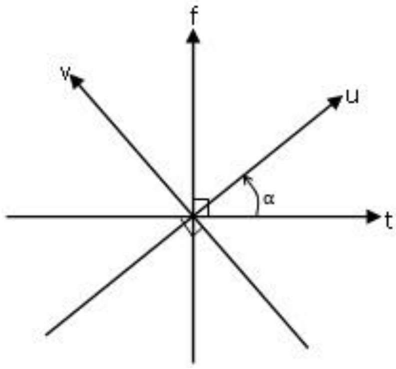

Fig. 1. The rotation angle of *α* in the *t-f* plane.

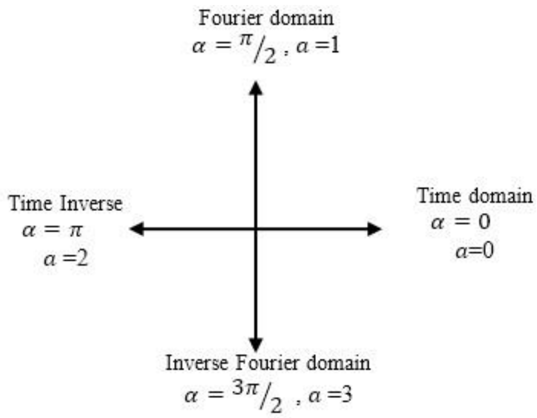

Fig. 2. Time-frequency plane in the FrFT domain.

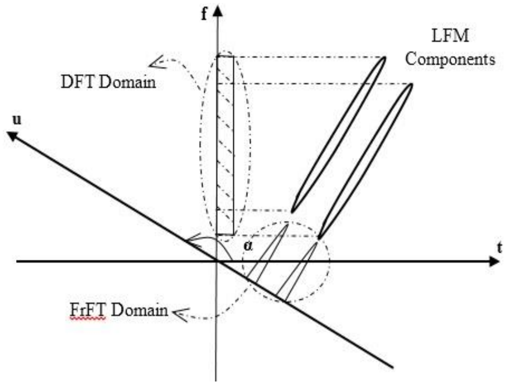

Fig. 3. The spectrum compression of chirp components in the FT and FrFT domains and component separation in the FrFT under optimal

The relation between the *t*-*f* variables (the old axes) and the *u*-*v* axes (the new axes) can be calculated using this matrix transformation:

$$\begin{bmatrix} u \\ v \end{bmatrix} = \begin{bmatrix} \cos\alpha & \sin\alpha \\ -\sin\alpha & \cos\alpha \end{bmatrix} \begin{bmatrix} t \\ f \end{bmatrix} \tag{4}$$

Similar to the FT, the properties of the FrFT has been studied in detail in many references, such as [9], [17], [18]. Further, the implementation method of the FrFT is discussed in [16], [19].

A. The Chirp Signal Processing Using FrFT

Chirp or LFM signal can be properly analyzed by exploiting the properties of the FrFT. Let $s(t)$ be an LFM signal and let $\varphi(t)$ and $\varphi'(t)$ be the instant phase and frequency of the LFM signal, respectively, as defined below:

$$s(t) = \exp(At^2 + Bt + C) \tag{5}$$

$$\varphi(t) = At^2 + Bt + C \tag{6}$$

$$\varphi'(t) = 2At + B \tag{7}$$

According to (7), due to the slope of the time-frequency characteristic of the chirp or LFM signal, such signals can be effectively processed using the FrFT. Fig. 3 demonstrates the energy distribution of two chirp signals located at two close time instants with the same chirp rate in the time-frequency (t-ω) plane.

As it can be observed, after applying the FT to these two signals, the obtained spectrums from the signals in the frequency domain, ω, have a significant overlap and the frequency components of the signals are not separable. Conversely, after applying the FrFT under an optimum rotation, α, the frequency components of the signals in the FrFT domain, has no interference on the u axis; hence, they are separable. Therefore, an order of FrFT (order a) can be found such that the signals are completely compressed. Thus, to compress a signal in the FrFT domain, finding an optimal transformation order is necessary.

When a chirp signal with the general form presented in (5) is considered, the optimal order of transformation for compressing the signal using the FrFT after sampling the signal can be determined using (8) [19]:

$$a_{opt} = -\frac{2}{\pi}\tan^{-1}\left[\frac{f_s^2/m}{2A}\right] \tag{8}$$

where f_s represents the sampling frequency, m denotes the number of samples and $2A = K_a$ denotes the chirp rate. Consequently, the FrFT can be applied under an optimal rotation to the signal formed by several chirp components, while the components remain separable.

III. The Azimuth Signal in SAR and the Imaging System Model

The azimuth SAR imaging model is presented in Fig. 4. For the sake of simplicity, we assume that the transmitted signal has the form of $p(t) = \exp(j\omega t)$, in which t is defined as the fast time. In this model, the radar moves along the orthogonal direction (i.e. the azimuth direction) and the earth is swept by the radar beam. The targets located within the beam's footprint return the scattered radar signal and they are received by the radar's antenna. To keep the analysis simple and to avoid unnecessary sophistication, the range of the targets, denoted by X_c, is assumed to be constant. Further, the number of targets located on line $x=X_c$ toward the azimuth is assumed to be n.

The slow time variable, whose variation forms the synthetic aperture, is assumed to be u. Moreover, the spatial frequency variable is k_u. In the general form, the targets' position in the azimuth direction is within the range $y_n \in [Y_c - Y_0, Y_c + Y_0]$. In addition, the returning echo from the target in the baseband is expressed by (9) [5]:

$$s(\omega,u) = \sum_n \sigma_n \exp\left(-2jk\sqrt{x_n^2 + (y_n + Y_c - u)^2}\right) \tag{9}$$

where $k=\omega/c$ represents the wave number; index n is used to denote the nth point-wise target. Parameter σ_n denotes the target reflection ratio, which, in practical sense, is a function of frequency ω and shows the distance between the target and radar. As it can be seen, this signal is formed, independent of the transmitted wave, $p(t) = \exp(j\omega t)$. If this baseband signal be the signal returned from a single target located in the middle of the target area, i.e. $(x_n, y_n) = (X_c, 0)$ then

$$s_o(\omega,u) = \exp\left(-2jk\sqrt{X_c^2 + (Y_c - u)^2}\right) \tag{10}$$

This signal is called the reference signal; as explained in these sections, it is used as a basis to form a matched filter.

In (9) the phase function, i.e. the exponential function exp(·), is called the spherical Phase Modulation (PM) signal, which is in fact a non-linear phase of u. By taking a derivative from (10), we get the instant spatial frequency of the Phase Modulation signal within the range $[-L, L]$ [5]:

$$K_{un}(u) = 2k\sin\theta_n(u);\ \theta_n(u) = \tan^{-1}\left(\frac{y_n + Y_c - u}{x_n}\right) \tag{11}$$

Here, $\theta_n(u)$ represents the viewing angle of the radar for the nth target. For all targets, we have x_n=X_c. To define the position of the targets along the azimuth direction, a matched filter in the spatial frequency domain, k_u, is required. Hence, the static phase estimation is applied and an FT is taken from (9) and (10) with respect to u [3], [5].

$$S(\omega,k_u)=\sum_n \sigma_n I_n(\omega,k_u)\exp\Big(-j\sqrt{4k^2-k_u{}^2}x_n - jk_u(y_n+Y_c)\Big) \tag{12}$$

$$S_0(\omega,k_u)=\exp(-j\sqrt{4k^2-k_u{}^2}X_c - jk_uY_c) \tag{13}$$

The Doppler bandwidth, which plays a fundamental role in determining the resolution of the azimuth SAR signal, can be estimated by

$$|\Omega_n| \approx \frac{4kL}{x_n}\cos^2\theta_n(0) \tag{14}$$

To reconstruct the target signal in practice, the reference signal should be used as a matched filter as follows:

$$\begin{aligned} F(k_u) &= S(\omega,k_u)S_0^*(\omega,k_u) \\ &= \sum_n \sigma_n I_n(\omega,k_u)\exp\big(-k_u(y_n+Y_c)\big) \end{aligned} \tag{15}$$

By taking an inverse spatial FT with respect to the spatial frequency, k_u, the cross-section range signal or the target's position along the azimuth direction is obtained [5]:

$$f(y)=\sum_n \sigma_n|\Omega_n|\exp(j\Omega_{nc}y)\mathrm{sinc}\left(\frac{1}{2\pi}|\Omega_n|y\right) \tag{16}$$

According to the geometry of the azimuth SAR imaging shown in Fig. 4, we have $Y_0+L \ll X_c$. Here, the Nyquist sampling interval in the slow-time domain can be expressed as the following approximate equation [5]:

$$\Delta_u \le \frac{X_c\ \lambda}{4(Y_0+L)\cos^2\theta_c},\quad \theta_c=\tan^{-1}\frac{Y_c}{X_c} \tag{17}$$

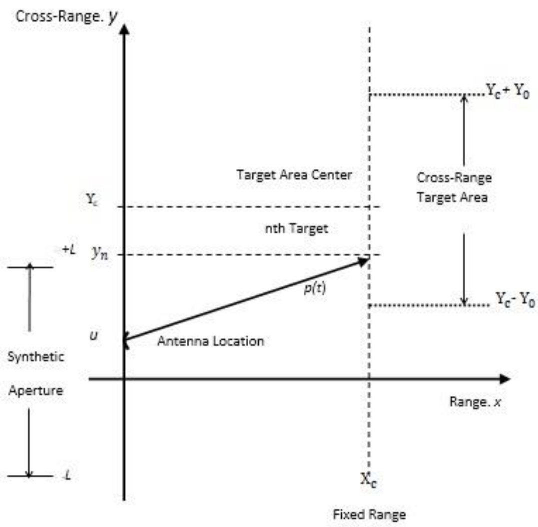

Fig. 4. The imaging system in SAR along the azimuth (cross range) direction [5].

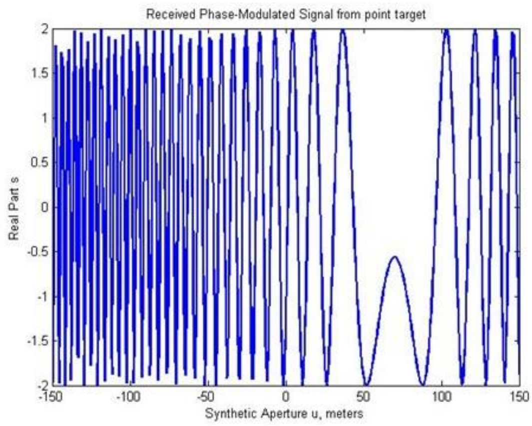

Fig. 5. The azimuth signal or phase modulation in the squint mode of a target with y_n=70 m.

TABLE I: IMPORTANT PARAMETERS OF THE AZIMUTH SIGNAL AND THE POINT-WISE TARGET

Parameter	Amount
Carrier frequency	200 MHz
Synthetic aperture length (2L)	800 m
Half-size of target area in cross-range domain (Y_0)	100 m
Target range (X_c)	1000 m
Cross-range of nth target (y_n)	70 m
Sample spacing of synthetic aperture signal (Δu)	0.7743 m
Sample spacing in spatial frequency domain (Δk_u)	0.0078 rad/m
Number of samples of synthetic aperture signal	1034

IV. SIMULATION AND RESULTS

In this section, first, the matched filter is simulated by applying the FFT to the azimuth signal received from a point-wise target. Then, the same simulation is conducted by applying the FrFT instead of the FFT. The 3 dB width of the amplitude of the compressed signal (expressed by (16)) is used as the comparison criterion for comparing the resultant resolutions of the two methods. The azimuth signal of a target located at (X_c, y_n)=(1000, 70) for the parameters listed in Table I is shown in Fig. 5.

To simulate the above equations in the distinct mode, first, (17) is employed to calculate the sampling rate (the Nyquist sampling interval in the slow-time domain) and the number of samples in the time domain m_u, as expressed as follows:

$$\Delta_u \le \frac{\pi}{2k\left[\dfrac{Y_0+L}{X_c}\right]}=\frac{X_c\ \lambda}{4(Y_0+L)} \tag{18}$$

$$m_u=\frac{2L}{\Delta_u} \tag{19}$$

Both methods use the above-mentioned parameters in the same way.

A. MF Based on FFT

In the FFT-based method, both signals represented by (9) and (10) are separately transformed using the FFT and then the results are multiplied. In the next step, the inverse FT of the multiplication result is calculated to reconstruct the azimuth signal in the slow-time domain and to determine the position of the targets along the synthetic aperture.

B. MSF Based on FrFT

Similar to the conventional FT-based simulation, in the proposed method based on the FrFT, the azimuth and reference signals are expressed by (9) and (10). As discussed in the previous sections, the time-frequency u–k_u characteristic of the azimuth signal expressed by (9) can be transformed into a new time-frequency characteristic under a given rotation $u_f - ku_f$ to achieve a desired compression factor for improving the resolution. The signal compression in the azimuth direction performed by applying matched filtering in the FrFT domain includes these steps:

- Calculating the optimum transformation order (a_{opt}): to calculate a_{opt}, the chirp rate $2A$, denoted by K_a, should be defined first. To do this, the Fresnel approximation is applied on the argument of PM signal (10) to yield an approximation as a second-order binomial equation (in the form of (6)) and then by taking a derivative, the Doppler instant frequency (in the form of (7)) and consequently the chirp rate is calculated. Substituting the sampling frequency, f_s, with $2\pi / \Delta_u$ in (8), and replacing m_u with the sampling rate, m, and using (20) for determining the chirp rate, the order of transformation, a_{opt}, is obtained from (8).

$$
\begin{aligned}
K_{un}(u) &= \frac{\partial}{\partial u}\left[-2k\sqrt{x_n^2+u^2}\right] \\
&= \frac{\partial}{\partial u}\left[-2k\left(x_n^2+u^2\right)^{\frac{1}{2}}\right] \\
&= \frac{\partial}{\partial u}\left[-2kx_n\left(1+\frac{u^2}{x_n^2}\right)^{\frac{1}{2}}\right] \\
&\approx \frac{\partial}{\partial u}\left[-2kx_n\left(1+\frac{u^2}{2x_n^2}\right)\right] = \frac{-2k}{x_n}u
\end{aligned}
\qquad (20)
$$

$$K_{un}(u) \approx \frac{-2k}{x_n}u$$

$$2A = K_a = \frac{-2k}{x_n} = \frac{-2k}{X_c}$$

  However, the calculated order of transformation might require a slight correction due to the pseudo-linear and non-stationary characteristics of the synthetic aperture. The final and accurate order of transformation is then yielded by applying a final correction step.

- Implementing the matched filer in the FrFT domain: After calculating $S(\omega, k_{uf})$ and $S_0(\omega, k_{uf})$ in the FrFT domain and under a_{opt} in accordance with the presented steps, the output matched filtering in the FrFT domain is calculated based on (15).
- The azimuth signal reconstruction in the synthetic aperture area (the slow-time domain): To reconstruct the signal, according to the definition of the inverse FrFT, an FrFT is taken from $F(k_u)$ under the transformation order of $a= -1$. Consequently, the azimuth signal in the synthetic aperture u_f is obtained representing the target position in the area (see Fig. 4).
- As it can be seen from Fig. 1, the FrFT rotates the signal characteristic by α degrees, and thus the sampling intervals on the old and the new axes differ by a cos(α) ratio. Therefore, an axis scaling should be applied to the new time axis after applying the inverse Fourier transformation transforming the signal back into the slow-time domain (the synthetic aperture area). The scaling, through which the position of the target on the synthetic aperture u is corrected, can be accomplished using (21):

$$\Delta_{uf} = \Delta_u \cos\alpha \qquad (21)$$

  where Δ_{uf} represents the retrieved sample intervals and Δ_u shows the sample intervals of the synthetic aperture.

C. Results

In comparison with other usual methods, the proposed method has two main differences. First, existing similar methods apply the inverse FrFT under the rotation of $-\alpha$ in the fourth step to reconstruct the signal in the slow-time domain to determine the exact position of the target at the synthetic aperture area. This method declines the compression factor of the reconstructed signal. Conversely, in the proposed method, the resultant compression of the reconstructed signal in the FrFT domain is preserved. Second, in usual methods, the signal compression using the FFT results in the POSP [3], [13]. However, in the proposed method the simulation is performed only in the non-stationary mode and only one squint angle (10.2 degree) was simulated in both stationary and non-stationary modes for comparison, as the results are presented in Fig. 6 and Fig. 7. As implied by the results demonstrated in Fig. 6 and Table II, the FFT-based method achieved the azimuth resolution of 0.96 m. Further, the amplitude of the first sidelobe is −12.8 dB. However, in the MSF-based method with transformation order of $a= -0.9809$ in the FrFT, the values for the same parameters are 0.55 m and −18 dB, respectively, which indicate improvement in the resolution; reduction in the side lobes area. Further, Fig. 7 shows the results of the compression of the echoed signal from the targets in the stationary phase mode in both methods. In this figure, the azimuth and amplitude of the first sidelobe based on the FFT were 0.92 m and −47.17 dB, respectively, while the resultant values of the parameters in the MSF-based method (with $a = -0.5790$) were 0.125 m and 40 dB, respectively. By comparing the results, it can be seen that the proposed method has a better performance in terms of stationary phase approximation than that of the FFT-based method.

Fig. 8 demonstrates the simulation results in terms of resolution and PSLR of the targets for different squint values with azimuth position of 70 m. The numeric values are given in Table II. As it can be seen, the MSF-based method significantly improves the non-stationary resolution and PSLR. This significant improvement of the side lobe areas after the azimuth signal compression stems from the non-linear time-frequency (instant frequency) characteristic of the signal, as it can easily be observed in (11). The mentioned equation is in fact a part of a sinusoidal function whose characteristic is approximated by applying a stationary phase approximation. However, for non-zero squint angles, the location of the target moves along the range direction and, duo to the $\exp(j\Omega_{nc}y)$ term, it varies with respect to the azimuth phase. This fact is evident when inspecting (15). In the broadside mode, the central Doppler frequency of the equation is almost equal to zero ($\Omega_{nc} \cong 0$). However, in the squint mode, the central Doppler frequency is non-zero, hence, a phase is added to the target's position in the azimuth direction that leads to higher variations of this characteristic with respect to the slow time. As a result, the received echo signal from the target becomes more non-stationary. Despite the existence of this challenge, the efficiency of the proposed method is evident from the results presented in Table II. Although both methods obtained close results for high squint angles, the proposed method functioned better than its counterpart in low squint angles. When the antenna squint is high enough that the sum of the signal phase and the antenna squint approaches 90 degree (or –90 degree), then the optimum transformation order occurs around a = 1 (or a =3 or a= –1), as seen in Fig. 8 (d). (a = –0.9979 ≈–1). In other words, FrFT and FFT will have the same results. The simulation results prove that the FFT method is not robust against squint angle variations. An additional benefit of the proposed method is its flexibility in processing the signals with a non-linear time or frequency characteristic so that an optimum transformation order can be found for each point of the characteristic at which the resolution is maximal. In other words, the proposed method is robust against squint signal variations and when the squint angle or the position of the target is changed, the method calculates an appropriate transformation order to maintain the PSLR and resolution at their desired levels.

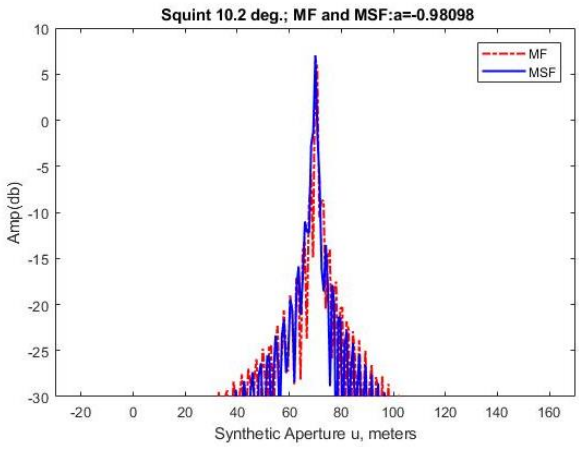

Fig. 6. Compression of the FFT- and FrFT-based methods without applying the POSP approximation.

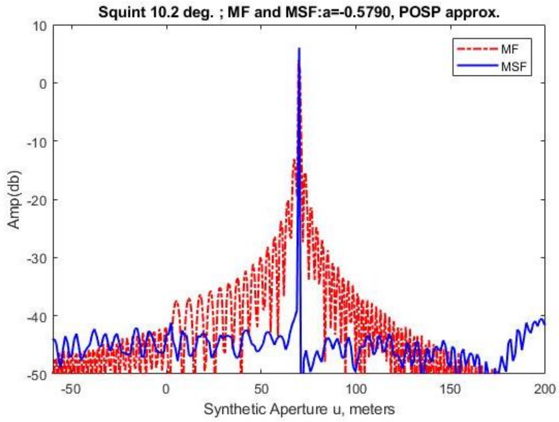

Fig. 7. Compression of the FFT- and FrFT-based methods under the POSP approximation.

TABLE II: DETAILED COMPARISON OF THE SIMULATION RESULTS

Squint (θ_c)	Method	The azimuth resolution (m)	PLSR (dB)
10.2 Degree	FFT POSP	0.92	-17.47
	FrFT POSP	0.125	-40
	FFT	0.96	-12.8
	FrFT	0.55	-18
20 Degree	FFT	0.76	-16.5
	FrFT	0.70	-17.2
30 Degree	FFT	1.4	-11
	FrFT	1.1	-15
45 Degree	FFT	2.4	-11.3
	FrFT	2.2	-12.3
60 Degree	FFT	3.3	-12.2
	FrFT	3.3	-11.63

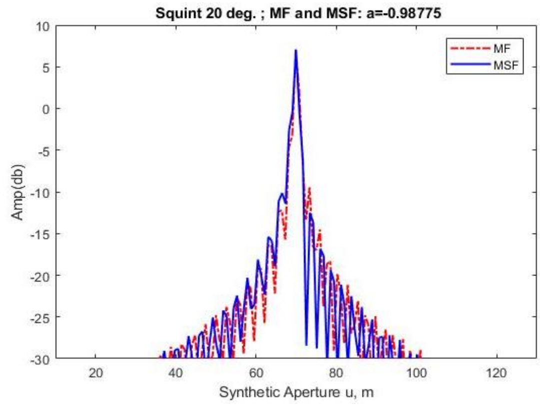

(a)

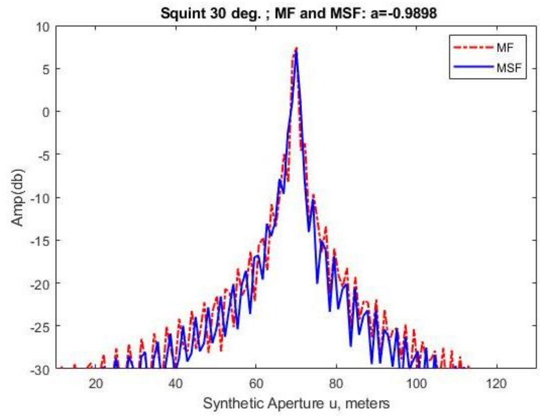

(b)

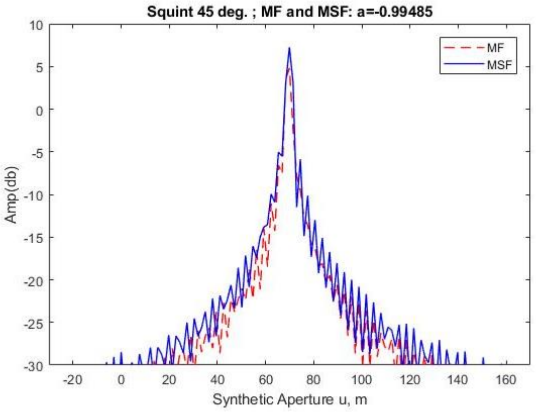

(c)

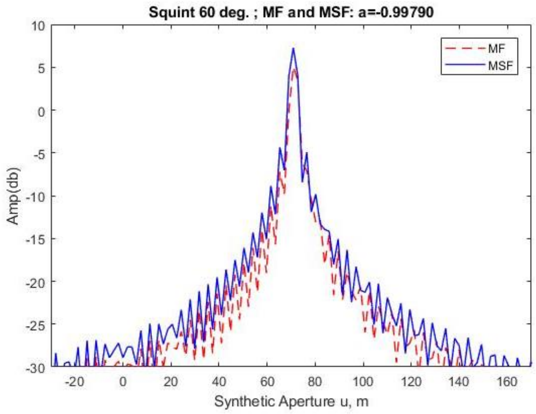

(d)

Fig. 8. Reconstruction of the azimuth signal and target location by FFT based method and FrFT based: (a) squint 20 deg. (b) squint 30 deg. (c) squint 45 deg. and (d) squint 60 deg.

Another important fact is that the transformation order (*a*) as a degree of freedom in the calculation allows to establish a tradeoff between resolution and side lobes amplitude. The simulation results indicate that the proposed method improves the overall resolution and reduces overall PSLR, while similar methods mostly reduce PSLR; no significant change is experienced in the resolution.

V. Conclusion

In this paper, a mathematical presentation of a general azimuth SAR imaging method and the azimuth signals in the squint mode were described and the related challenges were discussed. Then, the classic compression method based on the MF was presented and a novel method based on MSF was proposed to improve the azimuth resolution. Both methods then were simulated for stationary and non-stationary phase in the azimuth signal. The methods were evaluated in terms of resolution and PSLR with and without applying POSP approximation. Overall, the proposed method based on MSF has higher flexibility than the FFT-based method and showed higher robustness against variations in squint angle and target's position. The simulation results show that in the proposed method azimuth resolution and PSLR in low squats is improved at least 20% and 3 dB, respectively. In high squats, the results of the proposed method are the same as the FFT-based method. Consequently, the proposed method outperforms the traditional FFT-based method by improving SAR azimuth resolution and decreasing the sidelobes.

Conflict of Interest

The authors declare no conflict of interest.

Author Contributions

Farhad Sadeghi Almaloo conducted numerical simulation and wrote this paper. Assistant Prof. Majid Zarie gave simulation setting and reviewed this paper. Assistant Prof. Khodadad Halili and associate Prof. Jafaar Khalilpour gave comments and advises about this proposed method and provided critical feedback and helped shape the research, analysis and manuscript. All authors discussed the approach and results, contributed to the final manuscript and had approved it.

References

[1] Z. Ding, L. Liu, T. Zeng, W. Yang, and T. Long, "Improved motion compensation approach for squint airborne SAR," *IEEE Trans. on Geoscience and Remote Sensing*, vol. 51, no. 8, pp. 4378-4387, Aug. 2013.

[2] Y. Gao, Q. Lu, X. Liu, and Q. Chen, "A novel compensation approach for the range-dependent motion error based on time scaling," in *Proc. IEEE International Geoscience and Remote Sensing Symposium*, Valencia, 2018, pp. 6711-6714.

[3] I. G. Cumming, F. H. Wong, *Digital Processing of Synthetic Aperture Radar Data: Algorithms and Implementation*, MA, Norwood: Artech House, 2005.

[4] N. Levanon, E. Mozeson, *Radar Signals*, New York: Wiley, 2004.

[5] M. Soumekh, *Synthetic Aperture Radar Signal Processing with Matlah Algorithms*, New York: Wiley, 1999.

[6] W. Fan, M. Zhang, J. Li, and P. Wei, "Modified range-Doppler algorithm for high squint SAR echo processing," *IEEE Geoscience and Remote Sensing Letters*, vol. 16, no. 3, pp. 422–426, 2019.

[7] V. Namias, "The fractional order fourier transform and its application to quantum mechanics," *IMA Journal of Applied Mathematics*, vol. 25, no. 3, pp. 241–265, 1980.

[8] E. Sejdić, I. Djurović, and L. Stanković, "Fractional Fourier transform as a signal processing tool: An overview of recent developments," *Signal Processing*, vol. 91, no. 6, pp. 1351–1369, 2011.

[9] Y. Zhang, Y. Wang, *et al*, "A comprehensive survey on fractional fourier transform," *Fundamenta Informaticae*, vol. 151, no. 1–4, pp. 1–48, 2017.

[10] S. A. Elgamel, C. Clemente, and J. J. Soraghan, "Radar matched filtering using the fractional Fourier transform", in *Proc. Sensor Signal Process for Defence*, London 2010, pp. 1-5.

[11] A. S. Amein and J. J. Soraghan, "Azimuth fractional transformation of the Fractional Chirp Scaling Algorithm (FrCSA)," *IEEE Trans. on Geoscience and Remote Sensing*, vol. 44, no. 10, pp. 2871–2879, 2006.

[12] L. Dong, L. Huan, L. Hongqing, L. Guisheng, and T. Xiaoheng, "Focus improvement for high-resolution highly squinted SAR imaging based on 2-D spatial-variant linear and quadratic RCMs correction and azimuth-dependent Doppler equalization," *IEEE Journal of Selected Topics in Applied Earth Observations and Remote Sensing*, vol. 10, no. 1, pp. 168–183, 2017.

[13] C. Clemente and J. J. Soraghan, "Fractional range doppler algorithm for SAR imaging," in *Proc. 7th European Radar Conference*, 2010, pp. 248–251.

[14] M. G. El-Mashed, O. Zahran, M. I. Dessouky, M. El-Kordy, and F. E. A. El-Samie, "Synthetic aperture radar imaging with fractional

fourier transform and channel equalization," *Digital Signal Processing: A Review Journal*, vol. 23, no. 1, pp. 151–175, 2013.

[15] S. Chen, S. Zhang, H. Zhao, and Y. Chen, "A new chirp scaling algorithm for highly squinted missile-borne SAR based on FrFT," *IEEE Journal of Selected Topics in Applied Earth Observations and Remote Sensing*, vol. 8, no. 8, pp. 3977-3987, Aug. 2015.

[16] J. Ma, H Miao, X. Su, C. Gao, *et al.*, "Research progress in theories and applications of the fractional fourier transform," *Opto-Electronic Engineering*, vol. 45, no. 6, pp. 170747, 2018.

[17] R. Torres and E. Torres, "Fractional fourier analysis of random signals and the notion of alfa-stationarity of the Wigner–Ville distribution," *IEEE Trans. on Signal Processing*, vol. 61, no. 6, pp. 1555–1560, 2013.

[18] O. Akay and G. F. Boudreaux-Bartels, "Fractional convolution and correlation via operator methods and an application to detection of linear FM signals," *IEEE Trans. on Signal Processing*, vol. 49, no. 5, pp. 979–993, 2001.

[19] C. Capus and K. Brown, "Short-time fractional fourier methods for the time-frequency representation of chirp signals," *The Journal of the Acoustical Society of America*, vol. 113, no. 6, p. 3253, 2003.

Farhad Sadeghi Almaloo was born in Tehran, Iran. He received the B.S. degree from the Air University, Tehran, Iran, in 1998 and the M.S. degree from the Imam Hossein Comprehensive University, Tehran, Iran, in 2012, both in communication engineering. He is currently pursuing the Ph.D. degree at the Islamic Azad University, Science and Research Branch, Tehran, Iran. He is at present working as instructor in the khatam al-anbia (pbuh) University, Tehran, Iran His research interests include optical communications, coding theory, digital signal processing, digital image processing, and pattern recognition.

Majid Zarie received his bachelor's degree in Electrical-Electronics Engineering from the Shahid Rajaee Teacher Training University, Tehran, Iran and his Master's degree in Electrical-Electronics Engineering from the Imam Hossein Comprehensive University, Tehran, Iran. He received his Ph.D degree in Electrical-Electronics Engineering from the Malek Ashtar University of Technology, Tehran, Iran. He is at present working as assistant professor in the khatam al-anbia(pbuh) University, Tehran, Iran. His current research interests are optical communications, digital signal processing, and digital image processing

Khodadad Halili received his bachelor's degree from Shahid Sattari Aeronautical University, Tehran, Iran and MSc. from Iran University of Science and Technology, Tehran, Iran both in Electrical- Communication Engineering. He received his Ph.D. in Cyber Security from Supreme National Defense University, Tehran, Iran. He is at present as Assistant professor in the Shahid Sattari Aeronautical University. His research interest is around microwave passive and active device, communication and RF circuits design, information technology and cyber security.

Jafaar Khalilpour received M.S. and Ph.D. degrees from Tarbiat Modares University, Tehran, Iran, in 1998 and 2009, all in electrical engineering. He is at present working as associate professor in the khatam al-anbia (pbuh) University, Tehran, Iran. His research interests include electrical circuits modeling, electromagnetic issues of complex materials, and microwave components.